International Journal of Chemical, Materials and Biomolecular Sciences
ISSN: 2415-6620
Vol:9, No:1, 2015

Semiconductor Supported Gold Nanoparticles for Photodegradation of Rhodamine B

Ahmad Alshammari, Abdulaziz Bagabas

***Abstract*—**Rhodamine B (RB) is a toxic dye used extensively in textile industry, which must be remediated before its drainage to environment. In the present study, supported gold nanoparticles on commercially available titania and zincite were successfully prepared and then their activity on the photodegradation of RB under UV A light irradiation were evaluated. The synthesized photocatalysts were characterized by ICP, BET, XRD, and TEM. Kinetic results showed that Au/TiO_2 was an inferior photocatalyst to Au/ZnO. This observation could be attributed to the strong reflection of UV irradiation by gold nanoparticles over TiO_2 support.

***Keywords*—**Supported AuNPs, Semiconductor photocatalyst, Photodegradation, Rhodamine B.

I. Introduction

SECURING suitable water for drinking and irrigation purposes is an important issue in the whole global. Water purification and recycling, in addition, is a preventing measurement of environment contamination and a saving tool of water in arid places. Industries contribute significantly to environment pollution by various ways such as wastewater effluent [1], [2]. Textile industries, for instance, contaminate water by draining aqueous dye pollutant solutions [3]. Adsorption is a good treatment technique for the abatement of dye wastewater stream [4]. However, this technique generates waste solid, which requires further purification of the adsorbent materials and treatment of the separated pollutant. Therefore, such procedure increases the cost of water purification, but it would avoid us the landfill with solid wastes. Furthermore, depending on the nature of the adsorbent material, regeneration process may produce the adsorbent with its same original activity or less. The adsorbent may lose its activity after a certain number of recycling. Thus, with all these drawbacks of adsorption technique, advanced heterogeneous photocatalytic oxidation of dye pollutants emerges as an effective, economic alternative technique because of the complete destruction of the dye pollutant by the generated active oxygen-containing species under the illumination of UV-visible light to much less harmful products and of the easiness of photocatalyst separation and recyclability [5].

A. A. is with the National Nanotechnology Research Center, King Abdulaziz City for Science and Technology, P.O. Box 6076, Riyadh 114422, Saudi Arabia (phone: 966-11481-4285; fax: 966-11481-3671; e-mail: aalshammari@kacst.edu.sa).

A. B. is with the National Nanotechnology Research Center, King Abdulaziz City for Science and Technology, P.O. Box 6076, Riyadh 114422, Saudi Arabia (e-mail: abagabas@kacst.edu.sa).

Semiconductors have been widely used as photocatalysts in advanced photocatalytic oxidation technique. Depending on the band gap energy (Eg) of the semiconductor photocatalyst, either UV or Visible irradiation can be used for excitation and generation of exciton (electron-hole pair), needed for redox decomposition of pullotant. Titania, TiO2, and zincite, ZnO, have wide Eg of ~3.2 eV [6], making them appropriate absorbents of long wave ultraviolet light (UV A, 3.1-3.94 eV) [7]. However, their Eg is tunable by doping them with other semiconductor or metal nanoparticles. The doping process enhances their photocatalytic performance through charge separation and minimization or elimination of electron-hole recombination [8]. Metal nanoparticles such as gold act as electron drainage or electron donating whether the excitation is made by UV or visible irradiation [8].

Several studies have focused in promoting the photocatalytic performance of TiO2 and ZnO by doping with gold nanoparticles (AuNPs) e.g. [8]. However, there is a little bit or no studies comparing these two semiconductor supports and exploring their effect on AuNPs. Therefore, in this work we have tried to find out the effect of TiO2 and ZnO supports promoted with AuNPs on the photodegradation of rhodamine B (RB) in aqueous medium, under UV A light irradiation.

II. Material and Methods

A. Materials

Tetrachloroauric acid trihydrate ($HAuCl_4.3H2O$, ≥99.9% trace metal basis, Sigma-Aldrich), sodium citrate dihydrate (≥99%, FG, Aldrich), tannic acid (ACS reagent, Sigma-Aldrich), rhodam Fine B (≥95% HPLC, Sigma), titanium dioxide (purum, >99%, Fluka), and zinc oxide (99%, ACS reagent, Riedel-De Haen AG) were commercially available and were used without further purification. Deionized water (18.2 MΩ.cm) was obtained from a Milli-Q water purification system (Millipore).

B. Synthesis of Photocatalyst

The catalysts were prepared in two steps using the commercially available TiO_2 and ZnO as oxidic supports. The first step dealt with the preparation of the colloidal AuNPs by the reduction of $HAuCl_4$ in aqueous solution using 1 wt.% tannic acid and 1 wt.% sodium citrate. The second step involved the impregnation of the colloidal AuNPs with an oxidic support to obtain slurry, which was stirred for 2 hours at room temperature and then the excess solvent was removed by a rotary evaporator. The obtained solids were oven-dried at 120°C for 16 hours and then were calcined at 350°C for 5

hours in air. The loading of AuNPs was fixed at 1 wt.%. More details on the catalyst preparation are described elsewhere [9].

C. Characterization

The Au-content was determined by inductively-coupled plasma optical emission spectroscopy (ICP-OES). The BET specific surface areas were estimated by nitrogen physisorption method at -196ºC. X-ray diffraction (XRD) patterns were recorded for phase analysis on a Philips X pert pro diffractometer, operated at 40 mA and 40 kV by using CuKα radiation and a nickel filter, in the 2-theta range from 2 to 80º in steps of 0.02º, with a sampling time of one second per step. The morphology of the catalyst was explored by transmission electron microscopy (TEM, JEM-2100F JEOL). Carbon-coated copper grids were used for mounting the samples for TEM analysis. Solid-state ultraviolet-visible (UV-Vis) absorption and reflectance spectra for photocatalyst powder samples were recorded on a Perkin Elmer Lambda 950 UV/Vis/NIR spectrophotometer, equipped with a 150 mm snap-in integrating sphere for capturing diffuse and specular reflectance.

D. Photocatalytic Test

The photocatalytic experiments were carried out in a glass beaker containing 100 ml, 20 mgL^{-1} of RB solution and 100 mg of photocatalyst sample, using Luzchem Photoreactor. Before exposure to UV A light irradiation, the reaction mixture was magnetically stirred in the dark for 1 hour to ensure adsorption/desorption equilibrium of the dye on the photocatalyst surface. Afterwards, the reaction suspension was irradiated by 365-nm UV light at a power of 54.3 W/m^2. Aliquot samples were taken from the reaction mixture at every 20-minute interval, were centrifuged for photocatalyst separation, and then absorbance was recorded at λ_{max} of 554 nm using the UV/Vis/NIR spectrophotometer. The RB dye concentration of the samples was estimated using established calibration curve. The percentage of degradation of dye was measured by applying the following equation: %Degradation = $(C_0 - C)/C_0$ x 100, where C_0 is the initial concentration of RB dye and C is the equilibrium concentration of RB dye after irradiation.

III. Results and Discussion

A. Chemical Composition and N_2-Physisorption

ICP results (Table I) showed that the loading of AuNPs on ZnO and TiO_2 is in line with the nominal content of Au (1 wt.%). Table I displays also the BET specific surface areas and pore volumes of AuNPs supported on ZnO and TiO_2. The Au/TiO_2 photocatalyst has slightly higher BET surface area than the Au/ZnO photocatalyst, whereas undopedZnO and TiO_2 have similar surface areas. The surface area of supports decreased after impregnation with AuNPs. These results indicate that the AuNPs are highly dispersed on the support without any sintering effect. Such good dispersion is also confirmed by XRD and TEM, as shown later.

TABLE I
ICP and BET Surface Area Results of Au NPs over ZnO and TiO_2

Catalyst	ICP	BET surface area (m^2/g)		Pore volume (cm^3/g)
Au/ZnO	0.9	45*	39+	0.10
Au/TiO_2	0.9	47*	43+	0.12

B. XRD Phase Identification

XRD patterns of AuNPs supported on ZnO and TiO_2 are displayed in Fig. 1 The XRD pattern of Au/TiO_2 showed the presence of anatase phase, as verified by the appearance of diffraction peaks at 2θ values of 25.4º , 37.9º, 48.1º, 54.0º, and 55.2º corresponding to (101), (004), (200), (105), and (211) crystallographic planes of anatase, respectively. The diffraction peaks located at 2θ values of 31.84°, 34.52°, 36.33°, 47.63°, 56.71°, 62.96°, 68.13°, and 69.18° correspond to (100), (002), (101), (102), and (110) crystallographic planes of ZnO hexagonal wurtzite phase. In addition, Fig. 1 reveals that no diffraction peaks corresponding to metallic Au can be observed in Au/ZnO and Au/TiO_2. Such observation could be due to their high dispersion and their small size, lending a good support to the observed size of AuNPs by TEM (≤5 nm). On another hand, the XRD pattern reveals diffraction peaks corresponding to the supports only.

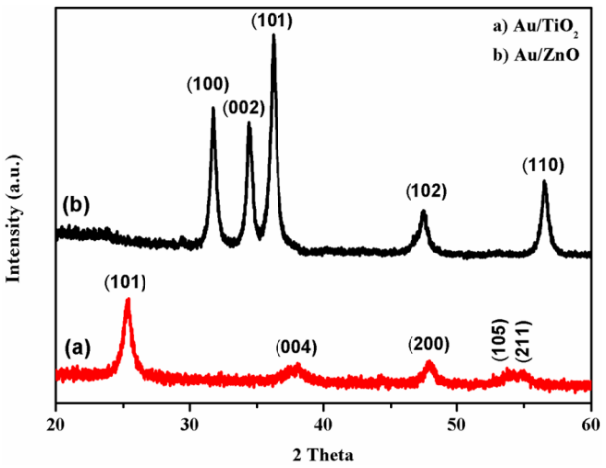

Fig. 1 XRD patterns of AuNPs supported on (a) TiO_2 and (b) ZnO

C. Size and Morphology of Au/TiO_2 and Au/ZnO

Representative TEM images of AuNPs supported on TiO_2 and ZnO are showed in Figs. 2 (a) and (b). The AuNPs are almost spherical and dispersed on the supports, while their particle size depends strongly on the nature of support. As shown in the inset of Figs. 2 (a) and (b), Au/ TiO2 and Au/ZnO resulted in a narrow particle size distribution in the range from 1-3 nm and 1-5, respectively. In addition, (HR)-TEM image (shown as insert in Fig. 2) enabled the observation of the crystal planes of AuNPs. The lattice d-spacing measured using HRTEM for Au/TiO2 and Au/ZnO is presented as in set images in Figs. 2 (a) and (b), respectively, and was compared with those of bulk Au. This figure illustrates HRTEM and corresponding fast Fouriertransform (FFT) and clearly shows that the inter planar spacing is visible and the gold particles are crystallized with an inter-planar

spacing of approximately 0.230 nm for Au/TiO2 and 0.227 for Au/ZnO. According to JCPDS no. 4-784 and the Bragg diffraction law, these values are very close to the bulk 0.235 nm d-spacing for the (111) plane in the face-centered cubic (fcc) phase of gold.

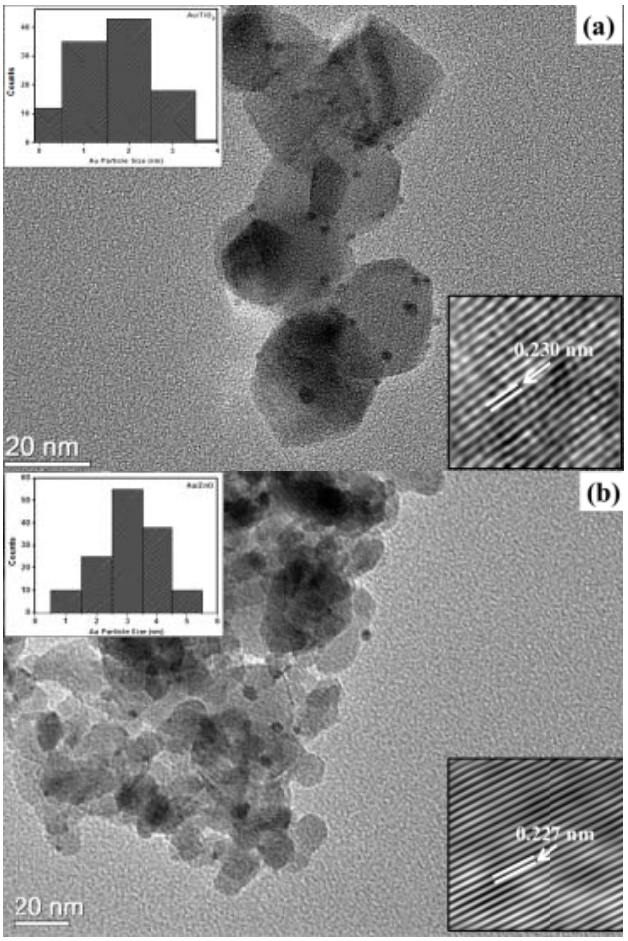

Fig. 2 TEM images of AuNPs supported on (a) TiO_2 and (b) ZnO. The inset images show a crystal planes of AuNPs in Au/TiO2 (in set (a)) and Au/ZnO (in set (b)). Histogram showing particle size of AuNPs supported on (in set (a)) TiO_2 and (in set (a)) ZnO

D. Solid-State UV-Vis Spectrophotometry

Figs. 3 (a) and (b) exhibit the UV-Vis absorption spectra of the undoped supports (ZnO and TiO_2) and the AuNPs-supported photocatalysts (Au/ZnO and Au/TiO_2). The broad surface plasmon resonance (SPR) band appears between 500 and 750 nm is due the presence of AuNPs on the ZnO and TiO_2 surfaces, as confirmed by XRD and TEM results. In contrast, the absorbance from 200 to 390 nm is due to ZnO or TiO_2. The position and shape of SPR depends on different factors such as particle size, shape, and dielectric constant of the medium [10].

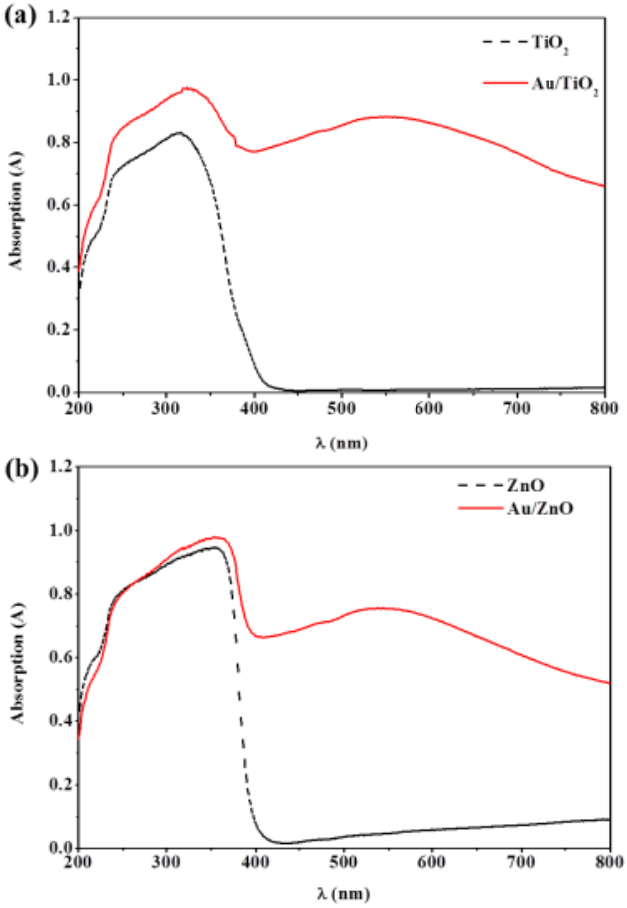

Fig. 3 UV-Vis absorption spectrum for AuNPs supported on (a) TiO_2 and (b) ZnO

The indirect band gap (Eg) estimation from these spectra for the undoped TiO_2 support and the AuNPs-supported on TiO_2 (Au/TiO_2) are illustrated in Fig. 4 (a), where the x-axis is the photon energy (E) in eV and y-axis is the square root of the product of absorption coefficient (α) and energy $(E\alpha)^{0.5}$. The direct band gap (Eg) estimation from these spectra for the undoped ZnO support and the AuNPs-supported on ZnO (Au/ZnO) are illustrated in Fig. 4 (b), where the x-axis is the photon energy (E) in eV and y-axis is the square of the product of absorption coefficient (α) and energy $(E\alpha)^2$. The Eg for undoped ZnO and TiO_2 were 3.27 and 2.90 eV, respectively. The indirect band gap value of TiO_2 was reduced to 2.51 eV after Au loading, while a slight decrease to 3.23 eV was observed in the direct band gap of Au/ZnO. Such observation implies that the optical properties of these materials are affected by the nature of the support. The reduction in the band gap of TiO_2 after loading AuNPs could be attributed to the "strong metal-support interaction, SMSI" because TiO_2 is well-known material exhibiting such phenomenon. This conclusion regarding the reduction of band gap due to SMSI could be supported by the higher absorption intensity of Au/TiO_2 in the visible light region in comparison to Au/ZnO (as shown in Figs. 3 (a) and (b). The increase in

absorption intensity upon Au loading over TiO_2 and ZnO implies higher photocatalytic activity under UV and visible light irradiation [8].

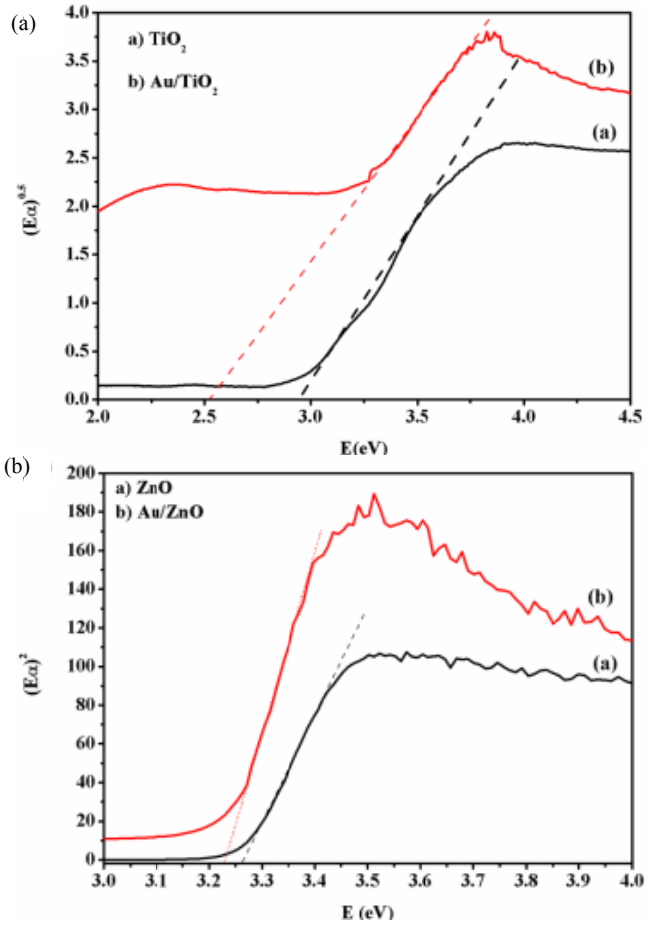

Fig. 4 Direct band-gap for AuNPs supported on (a) TiO_2 and (b) ZnO

Fig. 5 shows the UV-visible reflectance spectra of both Au/TiO_2 and Au/ZnO photocatalysts in the range of 200-800 nm. Au/TiO2 photocatalyst has higher reflectance percentage (R%) than Au/ZnO photocatalyst in the UV range from 226 nm to 382 nm, as shown in the inset of Fig. 5. Due to this fact, less UV A photons are absorbed by Au/TiO_2 photocatalyst, and hence, less exictons are generated and less photocatalytic activity are observed. In addition, the lesser reflectance percentage of Au/TiO_2 in the visible region as compared to Au/ZnO (as shown in Fig. 5) can also give another hint for the SMSI effect on the band gap of Au/TiO_2.

E. Photocatalytic Degradation of RB

Fig. 6 exhibits the UV-vis absorption spectra of a 20 mgL^{-1} Rhodamine B solution before and after UV A light irradiation in time interval of 20 min in the presence of (a) $Au/TiO_2$and (b) Au/ZnO as photocatalysts. Prior to irradiation with UV A light, an experiment was carried out in dark to ensure whether adsorption of dye occurred on the surface of catalyst or not. This experiment confirmed that slight decrease in concentration of RB was observed due to adsorption and found to be comparable for both Au/TiO_2 and Au/ZnO photocatalysts. According to Fig. 6 (a), the absorption peaks at 554 nm decreased with increasing irradiation time and finally vanished after 100 minutes of UV irradiation. In case of Au/ZnO photocatalyst (Fig. 6 (b), the characteristic absorption band of RB at 554 nm decreased significantly with increasing irradiation time without appearance of other absorption features. It can be seen from Fig. 6 (b) that the absorbance of RB almost disappeared after 80 minutes. As compared with the absorbance of RB with Au/ZnO, the photocatalytic activity of Au/TiO_2 showed a slower degradation which reached zero after 100 minutes. These results indicate that Au over ZnO has better photocatalytic activity than Au over TiO_2.

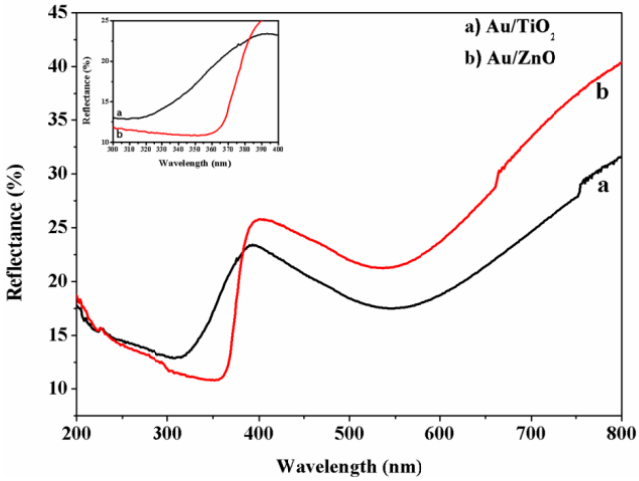

Fig. 5 UV-visible reflectance spectra of both Au/TiO_2 and Au/ZnO

Furthermore, we found that the photocatalytic degradation of RB in aqueous medium using undoped and Au-doped photocatalysts depended on the identity of the support, as evidenced by the degradation plot in Fig. 7. The RB photodegradation reactions over either undoped TiO_2 or undopedZnO are similar in the first 60 minutes with degrading ~73% of the present RB dye in solution. However, TiO_2 performance afterwards became better than that of ZnO until 160 minutes of reaction time. The RB degradation of ~98% efficiency was achieved over either TiO_2 or ZnO at 160 minutes of reaction and the degradation efficiency was constant afterwards with increasing reaction time. The stability of photocatalytic performance at and beyond 160 minutes could be attributed to the accumulation of the degradation products on the surface of the photocatalyst. On the other hand, doping both of TiO_2 and ZnO with 1 wt% AuNPs resulted in enhancing the RB photodegradation performance. The Au/TiO_2 photocatalyst resulted in 87% degradation efficiency after 60 minutes of the reaction while the Au/ZnO photocatalyst caused 96% degradation efficiency after 60 minutes. The enhancement in the photocatalytic degrading capability of both TiO_2 and ZnO could be attributed to the electron buffering of AuNPs, which in turn impede the

recombination of electron–hole pairs [8]. However, the lower performance of Au/TiO_2 than Au/ZnO could be due to the strong reflection of UV irradiation by AuNPs over TiO_2 support, as shown previously in Fig. 5. With increasing reaction time to 80 minutes, the degradation efficiency of Au/ZnO photocatalyst increased very slightly to 97% and stabilized at this value with the progress of reaction. On the other hand, the photocatalytic degradation capability of Au/TiO_2 gradually increased to 97% upon increasing reaction time from 60 minutes to 100 minutes, after which efficiency was maintained at this value. The plateau region of photocatalysts suggests the occurrence of deactivation by deposition of the reaction products on the photocatalyst surface.

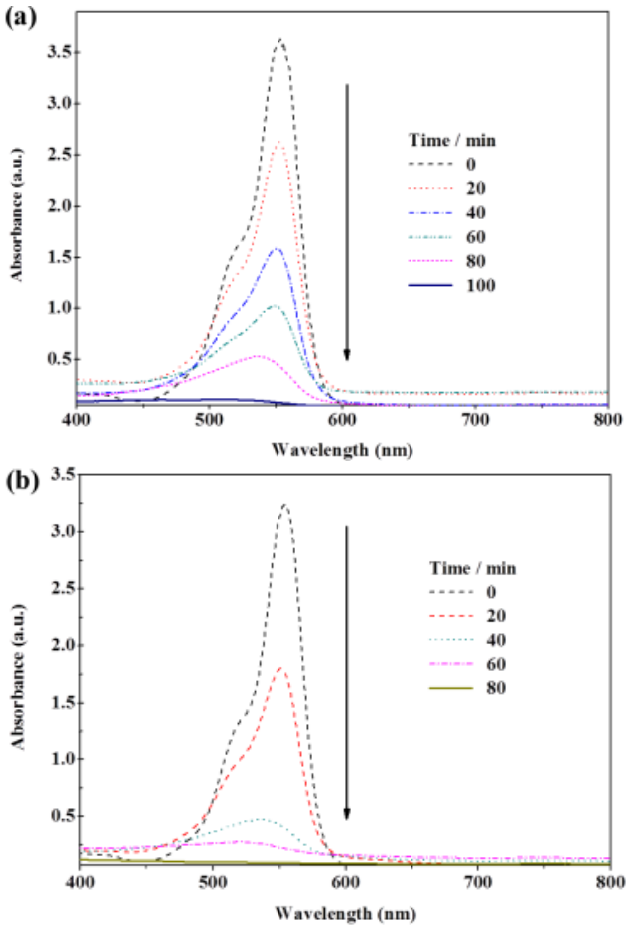

Fig. 6 Absorption spectra of RB at different time after UV irradiation using (a) Au/TiO_2 and (b) Au/ZnO as photocatalysts

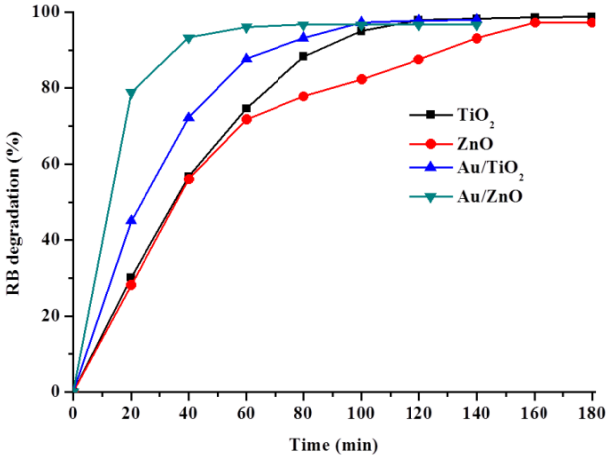

Fig. 7 Photocatalytic degradation of RB under UV irradiation catalyzed with TiO2 ZnO, Au/TiO2 and Au/ZnO

IV. Conclusion

Supported gold nanoparticles on commercially available titania and zincite were successfully synthesized and then their activity on the photodegradation of RB under UV A light irradiation were evaluated. The photocatalytic results showed that doping titania and zincite with 1 wt.% AuNPs accelerated the RB photodegradation over zincite and made it faster as ~2.7 times as that of undopedzincite, as ~2.0 times as that of undoped titania, and as ~1.8 times as that of titania supported AuNPs. The lower performance of titania supported AuNPs than zincite supported gold nanoparticles is due to the strong reflection of UV irradiation by gold nanoparticles over titania support. These findings explicitly reflect the key role of semiconductor support in the photocatalytic degradation of RB dye under UV A light irradiation.

Acknowledgment

This study was supported by King Abdulaziz City for Science and Technology (KACST) through project No. 29-280. We also thank Mr. Abdulaziz Arromaih for TEM analysis.

References

[1] S. Ahmed, M. G. Rasul, R. Brown, M. A. Hashib, "Influence of parameters on the heterogeneous photocatalytic degradation of pesticides and phenolic contaminants in wastewater: A short review" J. of Environm. Managem. vol. 92, pp. 311–330.

[2] R. Lilja, S. Liukkonen, "Industrial hazardous wastes in Finland – trends related to the waste prevention goal"*J. Clean. Prod*. vol. 16, pp. 343–349. 2008.

[3] N. M. Mahmoodi, M. Armani, N. Y. Lymaee, K. Gharanjig, K., "Photocatalytic degradation of agricultural N-heterocyclic organic pollutants using immobilized nanoparticles of titania" J. Hazard. Mater. vol. 145, pp. 65–71. 2007. 2001.

[4] C. Visvanathan, C., T. Asano, "The potential for industrial wastewater reuse, in: Vigneswaran S. (Ed.), Wastewater Recycle, Reuse, and Reclamation, EOLSS, e-book, 2009, pp. 299–317.

[5] A. Bagabas, M. Gondal, A. Dastageer, Z. Yamani, M.Ashameri, "Laser-induced photocatalytic inactivation of coliform bacteria from water using pd-loaded nano-WO3". Stud. in Surf. Sci. and Catal., vol. 175, pp. 279–282. 2010.

[6] K. Reddy, S.Manorama, A. Redd, "Band gap studies on anatase titanium dioxide nanoparticles" Mater. Chem. Phys. vol. 78, pp. 239–45, 2002.
[7] K. Rajeshwar, J. G. Ibanez, G. M. Swain, "Electrochemistry and the environment" J. Appl. Electrochem. vol. 24, pp. 1077–1091. 1994.
[8] H. Yu, H. Ming, J. Gong, H. Li, H. Huang, K. Pan, Y. Liu, Z. Kang, J. Wei, D. Wang, D., "Facile synthesis of Au/ZnO nanoparticles and their enhanced photocatalytic activity for hydroxylation of benzene" Bull. Mater. Sci. vol. 36, pp. 367–372, 2013.
[9] A. Alshammari, A.Koeckritz, V. N. Kalevaru, A. Bagabas, A., Martin, "Significant formation of adipic acid by direct oxidation of cyclohexane using supported nano-gold catalysts". ChemCatChemvol. 4, pp. 1330–1336, 2012.
[10] E. Ozbay, "Plasmonics: Merging photonics and electronics at nanoscale dimensions". Science vol. 331, pp. 189–193. 2006.

Ahmad Alshammari was born in Hail, Saudi Arabia on May 16, 1980. He received the B.Sc. degree in Chemistry from King Saud University, Riyadh, Saudi Arabia, in 2001, the M.Sc. degree in Designing Chemical Solutions from the University of Newcastle-upon-Tyne, Newcastle-upon-Tyne, U.K., in 2005, and then he studied chemistry at Leibniz Institute for Catalysis at the University of Rostock, where he completed his PhD thesis in the end of 2010 in the group of Prof. Axel Schulz and PD Dr. habil. Andreas Martin. In 2011, he joined the Petrochemical Research Institute, King Abdulaziz City for Science and Technology (KACST), Riyadh, where among other things he focused on the application of Heterogeneous Catalysis in different area. Presently he is Assistant Research Professor in the National Center for Nanotechnology, KACST. His principle research field is focused mainly on the application of nanomaterials and metal organic frameworks in different areas such as catalysis, photocatalysis, and energy. His scientific work has been published in more than 15 original publications. In addition, 6 patent applications have been granted in the last three years.

Dr. AbdulazizBagabas received his B.S. degree with Firs Honour in Chemistry from King Saud University in 1997 and his Ph.D. degree with Excellence in Inorganic Chemistry from Oklahoma State University in 2005. After completion of his undergraduate studies, he joined the Petroleum and Petrochemicals Research Institute (PAPRI), currently National Petrochemical Technology Center (NPTC), Materials Science Research Institute (MSRI), King Abdulaziz City of Science and Technology (KACST), where he is currently working Associate Professor. He was appointed an Honorary Research Associate at the department of Chemistry, University of Glasgow in 2006. He was also a visiting scholar at Chemistry Department, Northwestern University, Evanston, Illinois, USA, from 2011-2013. He has been recently got a visiting scholar position at the Department of Chemistry, University of California, Berkeley, California, USA. His research covers broad range of chemistry of materials. In particular, his research focuses on inorganic and organic syntheses, homogeneous and heterogeneous catalysis, environmental chemistry, nanotechnology, and corrosion. His work involves several joint researches with several national and international institutions. He has published more than 30 peer-reviewed articles, two book chapters, and 12 granted patents. He is a member of the editorial board of "Applied Petrochemicals Research" journal, published jointly by KACST and Springer, and a reviewer for various international journals.